Journal of Biomedical Optics

SPIEDigitalLibrary.org/jbo

Emerging concepts of laser-activated nanoparticles for tissue bonding

Paolo Matteini
Fulvio Ratto
Francesca Rossi
Roberto Pini

SPIE

Emerging concepts of laser-activated nanoparticles for tissue bonding

Paolo Matteini, Fulvio Ratto, Francesca Rossi, and Roberto Pini
Institute of Applied Physics "Nello Carrara," Italian National Research Council, via Madonna del Piano, 10-50019 Sesto Fiorentino, Italy

Abstract. We report recent achievements and future perspectives of minimally invasive bonding of biological tissues triggered by laser light. In particular, we review new advancements in the biomedical exploitation of near-infrared absorbing gold nanoparticles as an original solution for the photothermal closure of surgical incisions. Advanced concepts of laser tissue bonding involving the application of hybrid nanocomposites obtained by inclusion of nanochromophores into biopolymer scaffolds are also introduced. The perspectives of tissue bonding are discussed in the following aspects: (1) tissue bonding with highly-stabilized nanochromophores, (2) enhanced tissue bonding with patterned nanocomposites, (3) real-time monitoring of temperature distributions, (4) tracking of tissue regeneration based on the optical resonances of gold nanoparticles. [DOI: 10.1117/1.JBO.17.1.010701]

Keywords: laser; tissue repair; exogenous chromophores; nanoparticles; nanocomposites.

Paper 11429K received Aug. 8, 2011; revised manuscript received Oct. 25, 2011; accepted for publication Dec. 1, 2011; published online Jan. 19, 2012.

1 Laser Tissue Bonding

1.1 *Introduction*

The development of minimally invasive techniques holding the promise of reduced tissue pain and faster recovery is one of the leading trends in surgical medicine. In particular, the possibility to perform surgeries without sutures or staples is a valuable objective in view of minimally invasive clinical interventions.[1,2] One innovative approach for sutureless bonding entails the combination of laser light and an endogenous or exogenous optical absorber that may lie at the wound edges and mediate local generation of heat.[3] The most relevant endogenous absorbers are water, melanin, and haemoglobin, which may be excited by infrared and visible light. In order to enhance the localization of light deposition, it proves advantageous to use an exogenous chromophore and light at frequencies overlapping its optical extinction bands within a window where the competition from the endogenous absorbers is poor.[1,2] Finally, the thermal modification of the tissue is intended to generate new bonds between the wound edges, thus resulting in its closure.[3]

1.2 *Current Laser Tissue Bonding Strategies*

Nowadays, one of the preferred setups for sutureless laser-induced bonding involves the combination of near-infrared (NIR) light, which penetrates deep into the body, and an organic dye with optical extinction at the same frequencies.[3] Among the NIR-absorbing dyes proposed for laser bonding, Indocyanine Green (ICG)[4] has attracted very much interest from the medical community and is currently used to support a variety of surgical applications with a history of safety in humans.[5,6] In a typical laser-welding procedure, an aqueous solution of ICG is accurately spread between the tissue margins to be welded, while paying particular care to leave surrounding tissues unstained, thus avoiding their accidental absorption of laser light.[7] Then the wound edges are approximated and laser welding is performed under a surgical microscope by means of a NIR-emitting laser device (such as a diode laser) usually equipped with a fiberoptic delivery system. The heat produced upon irradiation with a NIR laser drives a thermal reorganization of the main tissue components, which results into the immediate closure and prompt repair of the wound.[3,8–10] This strategy proves particularly appropriate for those applications where suturing and stapling may prevent a regular healing process due to foreign-body reaction, such as, for example, in lamellar or penetrating keratoplasty, or for the treatment of thin tissues such as the lens capsular bag.[11–13] Additional advantages include reduced operation times and a substantial simplification of the overall surgery. The above procedure may be customized for specific applications by varying the irradiation conditions, such as laser power, emission mode, treatment duration, and mutual arrangement between the fiber tip and tissue.[14]

In addition, different and functional formulations of ICG may be employed, including liquid, semisolid, and solid solutions.[1,2] For instance, the chromophore may be homogeneously blended with a protein or polymer dispersion (e.g., albumin, fibrin, collagen, hyaluronan, etc.) that is pasted between the margins of the wound and finally irradiated with a NIR laser.[15–19] On heating, the ICG formulation coagulates and seals the wound, thus acting as a solder.[20] When the adhesion is mediated by the topical interposition of soldering material, this bonding technique is more properly referred to as laser soldering.[2] While liquid solders generally suffer from a high mobility of the absorbing chromophore during the soldering procedure, solid formulations exhibit low pliability, both of

Address all correspondence to: Roberto Pini, Institute of Applied Physics "Nello Carrara," Italian National Research Council, via Madonna del Piano, 10-50019 Sesto Fiorentino, Italy. Tel: +39 055 5225 303; Fax: +39 055 5225 305; E-mail: r.pini@ifac.cnr.it

0091-3286/2012/$25.00 © 2012 SPIE

which hamper the achievement of reproducible results.[2,21] In this context, the use of semisolid polymer formulations such as polycaprolactone (PCL) and chitosan in the form of flexible films and scaffolds is one hopeful alternative.[18,21–23] These materials, in addition to an intrinsic versatility in their fabrication process, hold the promise of good biocompatibility, biodegradability on a timescale of several days to months inside the body, and capacity to host functional chemicals, which attracts much interest for tissue repair and drug delivery purposes.[24,25] Moreover, some formulations exhibit antimicrobial and chemoactractant properties, which can support and accelerate the wound healing process.[26] In a recently proposed system, ICG molecules were loaded into silica nanoparticles, which are further dispersed with PCL and used in the form of semidry scaffolds.[27] This system proved advantageous in improving the control over the local dye concentration, which is important to ensure better heat dosimetry.

1.3 *Novel Tissue Bonding Strategies with Metal Nanochromophores*

Despite the thorough research work that has been performed by several international groups in *ex vivo* models and in *in vivo* animal models,[2,11,28,29] only a few of the proposed approaches have reached the preclinical and clinical phases thus far.[11,12,30,31] The reason for this gap has to be found in a lack of standardization in the tissue bonding procedure, mainly related to the use of conventional organic chromophores and, in turn, to a poor control over the heat deposition, as mentioned above.

Notable issues ascribed to the use of exogenous chromophores of common use in surgical practices such as ICG include a dependence of their structural and optical response on their biochemical environment and temperature, and a rapid degradation over time.[4,32–34] In addition, these molecules suffer from limited light extinction efficiency, photobleaching, and possible phototoxicity (e.g., generation of reactive oxygen species).[4,35] With this background, there have been conceived recent proposals to replace these organic chromophores by metal[36] and composite metal-coated bead[37] nanoscale transducers, which hold the promise to extend the range of application of tissue bonding.[21,38] Similar to the organic dyes, these nanoparticles can be formulated both in aqueous suspensions and after dispersion in a suitable protein or biopolymer scaffold.[3,21] In the latter case, the biochemical matrix is activated by the photothermal conversion from the embedded chromophores, ultimately adhering to its adjacent tissues.[1]

To the broad class of metal nanoparticles belong the so-called gold nanorods (cylindrical nanoparticles) and gold nanoshells (silica core, gold shell), which are the most efficient nanochromophores for photothermal applications in biomedicine disclosed thus far.[39,40] Typical extinction spectra of gold nanorods and gold nanoshells display characteristic features originating from collective electron oscillations or plasmon resonances and comprise a weaker band in the green (such as that found for gold nanospheres) and a fairly stronger band in the NIR.[41–43] The latter can be tuned throughout the NIR window in a controlled manner during the nanoparticles fabrication, by changing the aspect ratio (length divided by waist diameter) of gold nanorods or the core diameter to shell thickness ratio of gold nanoshells (Fig. 1).[40,43–45]

In turn, upon excitation with radiation from a NIR laser, these plasmon resonances undergo excitation and relaxation mainly through nonradiative channels. The interplay of physical and chemical properties of gold nanorods and gold nanoshells gives a number of favourable features,[21,40,41,46–49] such as: (1) possibility to modulate the geometrical and optical properties during fabrication; (2) a unique enhancement of the near field; (3) exceptional absorption (e.g., gold nanorods can provide absorption coefficients higher by up to five orders of magnitude than those of conventional absorbing dyes) and scattering (preferentially ascribed to gold nanoshells) efficiencies; (4) high stability in the body and thresholds before photothermal degradation; (5) broad versatility of conjugation with additional biochemical molecules including ligands, drugs, and genes; and (6) inertness in the body and negligible intrinsic cytotoxicity. For these reasons, these nanoparticles have been investigated as valuable contrast agents and sensitizers in a variety of diagnostic (e.g., optical and photoacoustic imaging and optical coherence tomography) and therapeutic (e.g., photothermal and photoacoustic microsurgery) applications[50,51] including laser bonding.

A few papers reporting the successful application of gold nanorods and gold nanoshells for tissue bonding have appeared in the recent scientific literature. For instance, Gobin et al. have demonstrated the use of a solder composed of bovine serum albumin (BSA) and gold nanoshells (~110 nm diameter and ~10 nm shell thickness) to successfully seal *ex vivo* muscular and *in vivo* skin tissue lesions.[37] These authors used continuous wave radiation generated by a diode laser emitting at 808 to 820 nm with a 14 to 20 W cm^{-2} intensity to achieve successful fusion with tensile strength equal to that of native tissues. Similarly, Nourbakhsh and Khosroshahi[52] realized the closure of 20-mm-long incisions performed on explanted skin samples mounted on an automatic programmable scanning system by using a diode laser (peak emission at 810 nm) running in continuous wave mode at an optimal intensity of 60 W cm^{-2}. Recently, our research group demonstrated the successful application of an aqueous suspension of gold nanorods for the direct welding of explanted lens capsular tissues.[53] Later substantial advancements have been obtained upon inclusion of gold nanorods into polysaccharide scaffolds.[21] In these systems the sugar chains enwrap the nanoparticles, thus creating a protective barrier against the physiological environment and enhancing their stability, durability, effectiveness, and biocompatibility. Preliminary investigations consisted of *in vivo* laser closuring of full thickness incisions performed in the carotid artery wall by means of a 810-nm diode laser in conjunction with the topical application of a composite gel of hyaluronan and gold nanorods (Fig. 2).[54] Irradiation of the wounds with a continuous intensity of 40 W cm^{-2} provided successful closure of their edges with sufficient strength to sustain blood pressure and ideal healing within a 30-day follow-up.

A further optimization of tissue repair procedures with gold nanochromophores consisted of the use of flexible materials with enhanced handiness and stability with respect to liquid or soluble solders such as those mentioned above. We recently proposed the introduction of a novel biocompatible material consisting of chitosan films containing gold nanorods, which can be readily bonded to biological tissues by photothermal activation.[55] These films are resistant, pliable, and stable in

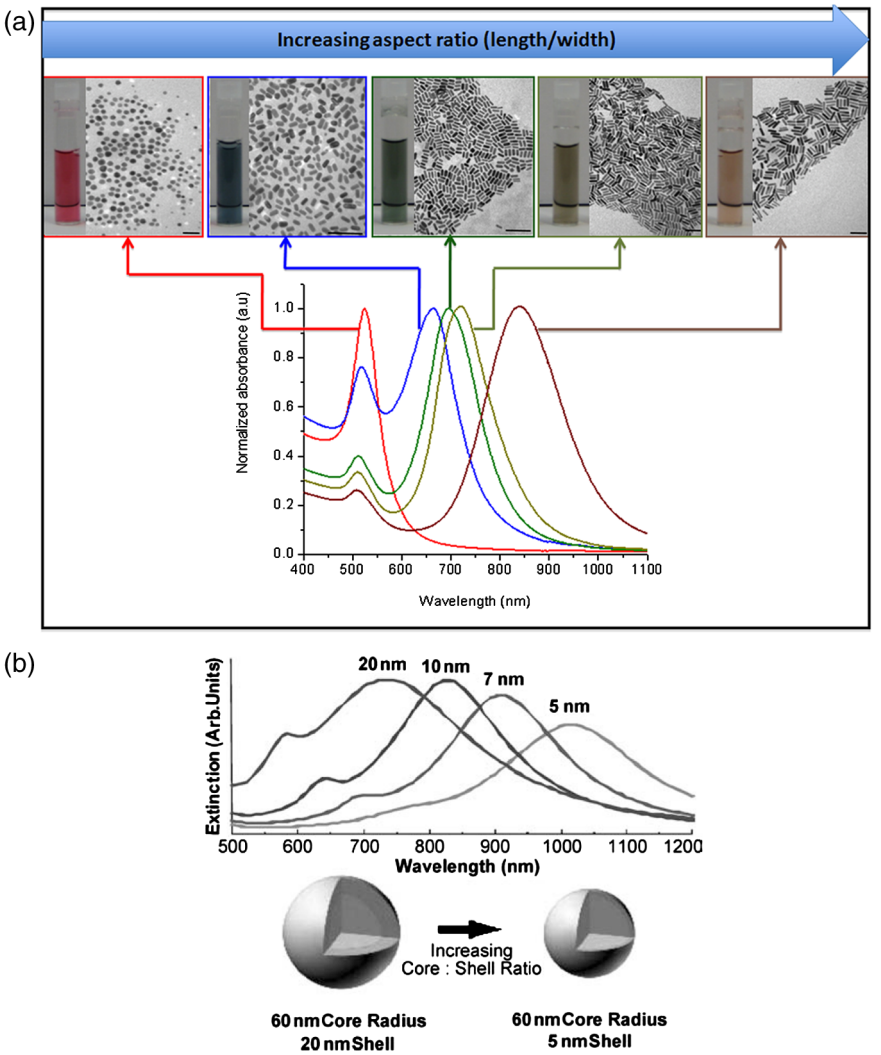

Fig. 1 (a) Gold nanorods of different aspect ratios display different colors which correspond to different absorption spectra (bar = 100 nm). Reproduced with permission from Ref. 46. (b) Optical tunability for nanoshells with a 60-nm silica core radius and gold shells 5, 7, 10, and 20 nm thick. The plasmon resonance red shifts with decreasing thickness of the gold shell (or increasing core to shell ratio). Reproduced with permission from Ref. 43. (Color online only.)

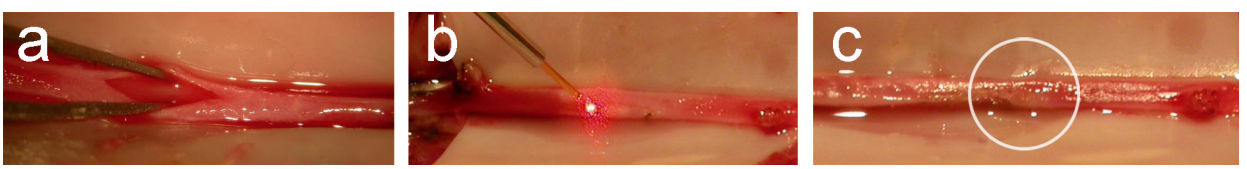

Fig. 2 Sequence of images recorded during the laser welding of a rabbit carotid artery with a gold nanorods/hyaluronan gel. (a) The artery is clamped and a 3-mm longitudinal incision is performed. (b) After application of the soldering formulation, the incision is treated with a 810-nm diode laser light. (c) Appearance of the sealed artery immediately after intervention. (Color online only.)

physiological conditions over time, while the chitosan matrix provides excellent control over the distribution and stability against aggregation of the nanoparticles, which translates into a dependable optical response and photothermal conversion [Figs. 3(a) and 3(b)]. Effective and reproducible adhesion of these films onto explanted carotid artery samples was achieved by means of contiguous spots of laser irradiation realized by gently bringing an optical fiber tip into contact with the films and delivering 810-nm diode laser pulses of 100 ms duration and 100 mJ energy, corresponding to 140 J cm^{-2} fluence at the outermost film surface [Figs. 3(c)–3(f)].[55]

Although beyond the focus of this paper, it is worth mentioning a different nanoparticle-inspired tissue bonding approach, which is based on magnetic instead of laser stimulation. This was recently proposed by Bregy et al.[56] with the final aim of reducing the effects of the inhomogeneities in the solder absorption and of increasing the radiation penetration through the tissue. The use of an albumin solder enriched with spherical superparamagnetic iron oxide nanoparticles (SPIONs) of 15 nm diameter allowed these authors to weld explanted blood vessels on application of 170-m radio waves[56] with strength comparable to that obtained with conventional suturing.

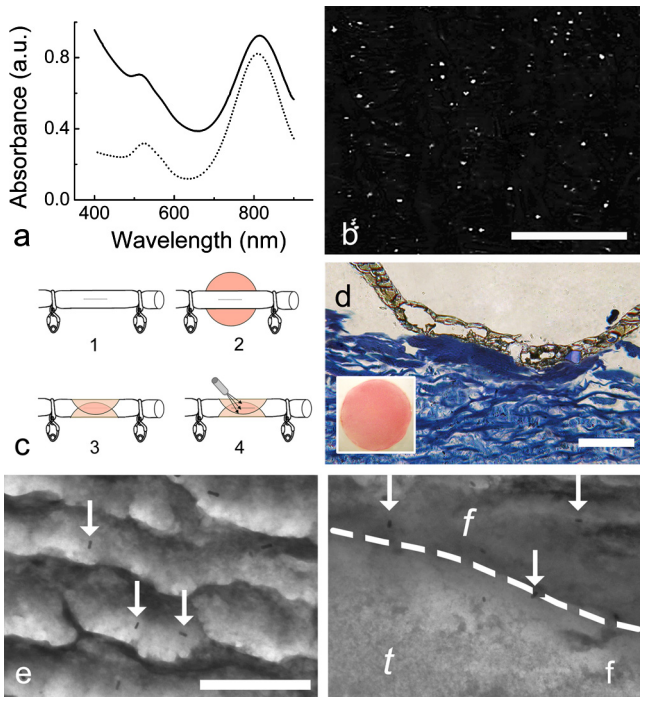

Fig. 3 (a) Comparison between the light extinction profiles of a hybrid gold/chitosan film (solid line) and the initial aqueous suspension of gold nanorods (dashed line). (b) SEM image of the gold nanorods distribution within a film sample (bar = 50 μm). A good balance between gold nanorods and chitosan concentrations provided for a homogeneous dispersion of particles within the polymer medium with an optical absorption profile closely resembling that of isolated nanoparticles. (c) Scheme of laser bonding of a hybrid gold/chitosan film to an arterial tissue—1: the artery is clamped proximally and distally and a 5-mm longitudinal cut is performed by means of a sharp-point; 2 and 3: a hybrid gold/chitosan film is topically applied onto the lesion and rolled all over the artery and 4: laser welded into its final position. Laser bonding is obtained by keeping the fiber tip in contact with the outer layer of the film and delivering single laser pulses of 100 mJ, 100 ms. (d) Toluidine blue stain of a cross-sectional slice of a film/tissue adhesion (bar = 100 μm). Comparison between TEM images of an untreated hybrid gold/chitosan film region (e) and of an adhesion region at the tissue/film interface (f) (bar = 500 nm; f = film; t = arterial tissue; gold nanorods are evidenced by arrows). A homogeneous adhesion characterized by close interdigitation between the biopolymer matrix and the external arterial wall is evidenced. (Color online only.)

2 Possible Developments and Perspectives

2.1 *Tissue Bonding with Highly Stabilized Gold Nanochromophores*

The positive reception of gold nanochromophores for important photothermal applications, such as the laser hyperthermia of cancer, is backed by their excellent photostability, which outclasses that of organic dyes. However, tissue bonding may require unusually high laser fluences (well above 10 W cm^{-2}), which may challenge the shape durability of these nanoparticles. For instance, already well below the melting point of bulk gold, gold nanorods tend to transform into stable gold nanospheres on laser excitation or thermal bathing,[57,58] which may result from surface diffusion[59,60] and immediately translate into a loss of plasmon resonances and light extinction in the NIR window. Figure 4(a) displays the appearance of a chitosan film loaded with gold nanorods and irradiated through its central spot under conditions that may be required for tissue bonding. Already after a few seconds, this spot is seen to undergo a visible change in color from purple to green, which reflects the bleaching of the gold nanochromophores (i.e., their inhibition to further laser absorption). Similar dynamics have been reported for the gold layer surrounding the silica core of gold nanoshells as well, which was shown to degrade into byproducts such as small gold nanospheres with a large size distribution and little capacity to absorb NIR light.[61]

A possible solution may come from surface modification of the particles with a rigid inorganic or organic coating, in an attempt to impart enhanced stability and a mechanical constraint against photothermal reshaping.[41] For instance, deposition of a silica shell around gold nanorods [e.g., Fig. 4(b)] was shown to substantially delay the deformation of gold nanorods in front of NIR laser pulses in the second-to-nanosecond timescales.[62–64] Similarly, a carbon or polymethylmethacrylate coating was reported to significantly improve the photostability of gold nanoparticles.[65,66] The possibility to sustain high local temperatures is expected to enable better stability of the photothermal conversion and thus increase the overall reproducibility of tissue bonding. In addition, highly stable nanochromophores shall be less prone to laser-induced decomposition into small fragments,[66] whose presence may be undesirable *in vivo*. In fact, previous cytotoxicity studies provided evidence for cell death by necrosis or apoptosis when using clusters of few gold atoms around 1.4 nm in size,[46,67] which become negligible for gold nanoparticles of larger size.[46,68–70]

2.2 *Enhanced Tissue Bonding with Patterned Nanocomposites*

Further optimization of the tissue bonding technology may be achieved by the use of patterned nanocomposites. By this phrase we intend the fabrication of well-defined and functional particle geometries and distributions inside a composite formulation.[71,72] One example of patterned nanocomposites includes matrices

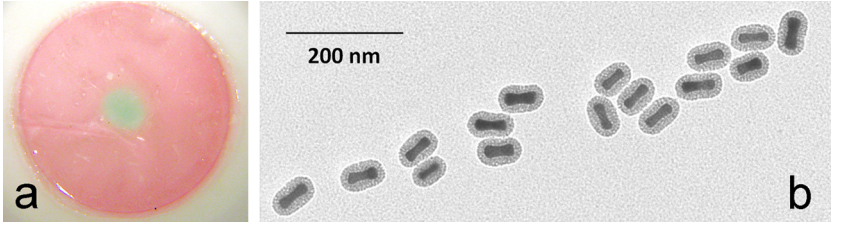

Fig. 4 (a) $A \sim 1$ cm diameter gold nanorods/chitosan film after exposure to 18 W cm^{-2} 810 nm laser light, which is typical for laser bonding. Note the change in color at the 2-mm-diameter central spot under irradiation. (b) Representative TEM micrograph of silica-coated gold nanorods, which may benefit from additional stability. (Color online only.)

with a gradient of optical absorbance along their length. These shall find application as laser-activated inserts inside an accidental wound or surgical incision. Indeed, the deeper the nanochromophore inside the cut, the larger the absorbance that is needed in order to produce an effective photothermal response, which is due to the light attenuation from the upper layers.[73] While the fabrication of durable graduated inserts with organic dyes remains a challenge,[23] this may be achieved for instance by subjecting gold nanorods embedded into a polymer strip to a suitable temperature gradient in order to modulate the particle's transformation along its length and so the spectrum of plasmon resonances.[65]

2.3 *Real-Time Temperature Monitoring by Optoacoustic Tomography during Tissue Bonding*

Subtle temperature dynamics inside the tissue critically affect the closure of a wound.[74–76] Indeed, the temperature increase needs to be high enough to trigger particular thermal processes[2,3] yet without inducing irreversible thermal damage, with a narrow window of optimal conditions.[77,78] Nowadays commercially available systems that enable a real-time, noninvasive monitoring of temperature dynamics in the clinical practice are based on infrared detectors such as thermocameras, which provide the spatial distribution and temporal evolution of temperature with very decent resolution. Unfortunately, this approach only provides a superficial temperature detection, which prevents fundamental insight into the temperature distribution inside the target. To overcome this restriction, analytical models based on the solution of the bioheat equation in a two- or three-dimensional domain are used to approximately track the temperature evolution deep inside the tissue.[3,75] However, use of these models is very delicate, due to the great complexity of biological tissues with their heterogeneous composition and subtle dissipative pathways. Valuable alternatives are represented by magnetic resonance imaging (MRI)[79] and ultrasound imaging,[80] which provide for a direct real-time monitoring of the temperature rise within biological tissues subject to photothermal treatments without the need for numerical postprocessing. However, while MRI does not hold much promise to become a routine tool for monitoring thermal effects deep in the body,[81,82] efficient equipment for ultrasonic detection of temperature in the clinical practice is not yet available.[83]

A recent and powerful alternative is nowadays represented by optoacoustic tomography (OAT), also called photoacoustic tomography (PAT), which is based on photoacoustic conversion (i.e., the generation of pressure waves and emission of ultrasound on absorption of light energy, preferably under thermal and stress confinement conditions).[84] OAT/PAT combines optical contrast based on absorption of NIR optical energy and detection of resulting acoustic pressure propagating as ultrasonic waves, resulting in a much higher lateral and depth resolution than pure ultrasonography and higher sensitivity with respect to MRI.[85–87] Due to the inherent optical contrast between cancerous and healthy tissue, OAT/PAT has originally found application in identifying cancerous lesions.[88–90] More recently, OAT/PAT has been proposed to measure temperature profiles by tracking thermally induced changes in thermoelastic properties and photoacoustic signal amplitudes (Fig. 5).[91–94] In this

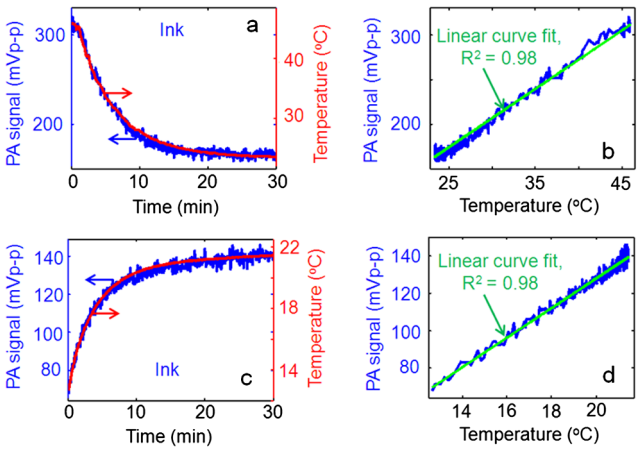

Fig. 5 (a) Photoacoustic (PA) signal and actual temperature of a source sample (diluted black ink solution with $\mu_a = 30\ \mathrm{cm}^{-1}$) as the heated sample was allowed to come to room temperature. The linear relationship between temperature and PA signal proves potential for real-time temperature sensing, (b) PA signal versus temperature from (a). The green line is a linear fit with an R_2 of 0.98. (c) PA signal and actual temperature of an initially cold sample warming up to room temperature, (d) PA signal versus temperature from (c). Again, the green line is a linear fit with an R_2 of 0.98. Reproduced with permission from Ref. 92. (Color online only.)

context, gold nanoparticles have been proposed as effective contrast agents for image-guided therapy based on photoacoustic imaging.[90,95] Once irradiated with pulsed laser light at low average power, these particles act as very local heat sources with temperature rapidly fading away with distance,[96] thus capable of triggering the photoacoustic conversion without interfering much with the overall tissue temperature. At present OAT/PAT represents a promising candidate to precisely monitor temperature changes during chromophore-enhanced photothermal therapies.[91] We anticipate a future involvement of OAT/PAT in the real-time guiding of photothermal tissue bonding with nanochromophores or nanocomposites. The possibility to simultaneously implement both techniques by the use of the same particles and with an endoscope will provide further benefits for extreme surgeries including the laser welding of gastrointestinal, urological, or intracranial tracts.

2.4 *Tracking of Tissue Regeneration Based on the Optical Resonances of Gold Particles*

A key concept to take full advantage of gold nanoparticles for tissue bonding is the tunability of their optical properties, as it was already mentioned in Sec. 1.3 and Fig. 1, which makes these new chromophores particularly attractive for theranostic applications.[97] In order to expand this point, Fig. 6 displays a collection of simulations of the light absorption (uppermost curves) and scattering (lowermost curves) cross sections for prolate elliptical gold nanoparticles in water with parameters representative of typical gold nanorods. As is shown, the two contributions of light extinction (scattering and absorption) of the particles can be modulated in amplitude and position throughout the visible NIR region by changing their size (volume) and shape (aspect ratio). As a rule of thumb, smaller nanoparticles are ideal for OAT/PAT and photothermal treatment procedures as light absorption dominates, while larger nanoparticles exhibit higher

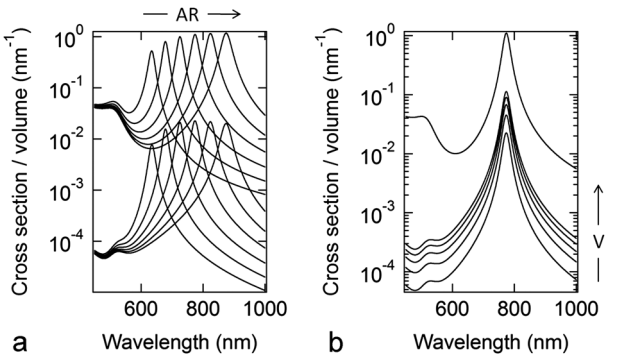

Fig. 6 Simulations obtained from Gans dipolar approximation,[98–100] and implemented with the analytical gold dielectric function given by Etchegoin et al.[101], which describe the light absorption (upper curves) and scattering (lower curves) cross sections from prolate elliptical gold nanoparticles with different shape (a) and size (b). (a) Variation of the optical properties of gold nanoparticles with the same volume $V =$ 1000 nm^3 and different length/diameter ratios (i.e., aspect ratio [AR]) from 2.5 to 5 in steps of 0.5 from left to right. The plasmon band in the NIR window progressively gains intensity and red-shifts with AR. (b) Effect of a constant AR = 4 and different volumes from 1000 nm^3 to 5000 nm^3 in steps of 1000 nm^3 from the low to the high scattering bands (the absorption bands scale with V in Gans models and so the absorption profiles overlap with each other in the normalization given in this figure). The principal bias is an increase of the ratio of light scattering to absorption with volume.

scattering efficiency, which may be preferable for specific optical imaging applications including optical coherence tomography (OCT).

OCT provides noninvasive imaging of living tissues with penetration depth in the low millimeter range and spatial resolution in the low micron range, which is superior to standard clinical methods of noninvasive imaging such as ultrasonography and MRI.[102] Highly scattering gold nanoshells (119 nm diameter, 12 nm shell thickness) have been shown to enhance OCT contrast *in vivo*.[51] In this example, both imaging and photothermal therapy have been performed with a single particle formulation designed for both scattering and absorption.[103] Different OCT modalities are based on differential absorption or backscattering albedo (the ratio of backscattering to total extinction), which offer the advantage of producing contrast in tissues with high turbidity.[104] In this context it is the absorption properties of plasmonic nanoparticles that are concerned and should prevail in comparison with the case of the conventional backscattering OCT modality.

The twofold functionality of gold nanoparticles as both photothermal transducers to trigger tissue repair and contrast labels for biomedical diagnosis is well suited to provide for breakthrough insight into tissue bonding applications. Resonant imaging based on gold nanoparticles dispersed at the weld site will be useful to track the progress of the wound healing process in the period that follows the tissue bonding intervention. The low diffusivity of gold particles through the tissue matrix with respect to that of organic chromophores (e.g., $\sim 10^{-8}$ cm^2 s^{-1} for 100-nm gold nanoparticles[105] as compared with $\sim 10^{-6}$ cm^2 s^{-1} for ICG[106] through connective tissues) implies a long-term permanence of the former *in situ*, while the latter are cleaned from the body within two to three days, which generates intense interest for their use for tissue monitoring during the follow-up period. This tendency can be amplified by increasing the nanoparticles size.[105] Previous studies have demonstrated the presence of 40-nm gold nanoparticles interdispersed within the extracellular matrix up to at least 30 days after a tissue bonding intervention (Fig. 7).[21,54] In addition, the use of functionalized particles capable of labeling different cell-surface factors or extracellular matrix biomarkers is expected to confer specificity to a particular biophysical or biochemical response occurring during tissue regeneration such as fibroblast migration, collagen deposition, and self-organization, and provide information on the evolution of these processes.[107,108]

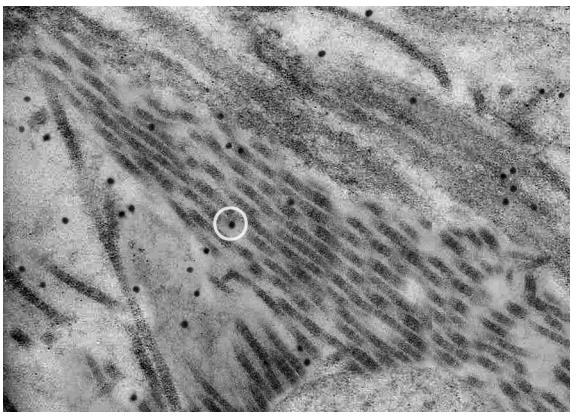

Fig. 7 TEM micrograph (4.2×3.0 μm^2) of a closured rabbit carotid artery after a 30-day follow up from laser bonding with gold nanochromophores.

3 Summary

Recent progress in the design and synthesis of novel nanoparticles with versatile optical response holds much potential to improve the current technology of tissue bonding based on organic dyes and extend its range of application. In this context, the combination of NIR-absorbing gold nanoparticles with a diode laser irradiation matching their plasmon absorption resonance represents an original solution. A further technical development involves the preparation of hybrid adhesives by dispersion of the nanochromophores into a biopolymer matrix in order to achieve stable laser-activatable nanocomposites, which provide for reproducible and resistant adhesion.

Possible future scenarios of successful bonding of biological tissues include engineering of nanochromophores with enhanced resistance against photothermal reshaping in order to preserve their characteristic plasmon resonances against high laser fluences, and of patterned nanocomposites with well-defined particle geometries, which may provide for thorough control over the laser excitation. In addition, the photoacoustic signal generated by gold nanoparticles at the weld site may be exploited to perform a real-time monitoring of local tissue temperature for guided photothermal tissue bonding. Another key concept to take full advantage of gold nanoparticles for tissue repair is the tunability of their optical response, which may enable resonant imaging based on different modalities (OAT/PAT and OCT) to track tissue regeneration during the follow-up period.

While gold nanoparticle—mediated photothermal bonding is at its very early stages, recent advancements in biomedical optics and nanomedicine let us expect a rapid development of this technology. Additional optimization strategies such as

those discussed above are needed in order to provide for full reproducibility and control over the photothermal process and tissue regeneration and ultimately build a standardized nanophotonics-based bonding procedure and devise surgeon-friendly protocols that may find application in the clinical practice.

Acknowledgments

This work has been partially supported by the Projects of the Health Board of the Tuscany Region "NANO TREAT" and "NANO-CHROM" and by the Network of Excellence "Photonics 4 Life."

References

1. R. Pini et al., "Laser tissue welding in minimally invasive surgery and microsurgery," in *Biophotonics*. Series: Biological and Medical Physics, Biomedical Engineering, L. Pavesi and P. M. Fauchet, Eds., pp. 275–299, Springer, Berlin (2008).
2. K. M. McNally, "Laser tissue welding," in *Biomedical Photonics Handbook* T. Vo-Dihn, Ed., CRC Press, Boca Raton, pp. 1–45 (2003).
3. P. Matteini et al., "Laser welding of biological tissue: mechanisms, applications and perspectives," in *Laser Imaging & Manipulation in Cell Biology* F. Pavone, Ed., Wiley-VCH, Berlin, pp. 203–231 (2010).
4. M. L. Landsman et al., "Light-absorbing properties, stability, and spectral stabilization of indocyanine green," *J. Appl. Physiol.* **40**, 575–583 (1976).
5. L. P. Kamolz et al., "Indocyanine green video angiographies help to identify burns requiring operation," *Burns* **29**, 785–791 (2003).
6. G. P. Holley et al., "Effect of indocyanine green intraocular stain on human and rabbit corneal endothelial structure and viability: An in vitro study," *J. Cataract Refractive Surg.* **28**, 1027–1033 (2002).
7. S. D. Decoste et al., "Dye-enhanced laser-welding for skin closure," *Lasers Surg. Med.* **12**, 25–32 (1992).
8. P. Matteini et al., "Microscopic characterization of collagen modifications induced by low-temperature diode-laser welding of corneal tissue," *Lasers Surg. Med.* **39**, 597–604 (2007).
9. P. Matteini et al., "Atomic force microscopy and transmission electron microscopy analyses of low-temperature laser welding of the cornea," *Lasers Med. Sci.* **24**, 667–671 (2009).
10. M. A. Constantinescu et al., "Effect of laser soldering irradiation on covalent bonds of pure collagen," *Lasers Med. Sci.* **22**, 10–14 (2007).
11. F. Rossi et al., "Laser tissue welding in ophthalmic surgery," *J. Biophotonics* **1**, 331–342 (2008).
12. F. Rossi et al., "'All laser' corneal surgery by combination of femtosecond laser ablation and laser tissue welding," in *Handbook of Photonics for Medical Science* V. V. Tuchin, Ed., CRC Press, Taylor & Francis Group, London, pp. 799–810 (2010).
13. R. Pini et al., "A new technique for the closure of the lens capsule by laser welding," *Ophthalmic Surg. Laser Imag.* **39**, 260–261 (2008).
14. V. L. Martinot et al., "Determination of efficient parameters for argon laser-assisted anastomoses in rats - macroscopic, thermal, and histological-evaluation," *Lasers Surg. Med.* **15**, 168–175 (1994).
15. B. Ott et al., "Intraluminal laser light source and external solder: In vivo evaluation of a new technique for microvascular anastomosis," *Lasers Surg. Med.* **35**, 312–316 (2004).
16. A. Puca et al., "Diode laser-assisted carotid bypass surgery: an experimental study with morphological and immunohistochemical evaluations," *Neurosurgery* **59**, 1286–1294 (2006).
17. A. Lauto et al., "Laser-activated solid protein bands for peripheral nerve repair: an vivo study," *Lasers Surg. Med.* **21**, 134–141 (1997).
18. A. Bregy et al., "Solder doped polycaprolactone scaffold enables reproducible laser tissue soldering," *Lasers Surg. Med.* **40**, 716–725 (2008).
19. B. S. Sorg and A. J. Welch, "Tissue welding with biodegradable polymer films-demonstration of acute strength reinforcement in vivo," *Lasers Surg. Med.* **31**, 339–342 (2002).
20. K. M. McNally et al., "Photothermal effects of laser tissue soldering," *Phys. Med. Biol.* **44**, 983–1002 (1999).
21. F. Ratto et al., "Gold nanorods as new nanochromophores for photothermal therapies," *J. Biophotonics* **4**, 64–73 (2011).
22. A. Lauto et al., "In vitro and in vivo tissue repair with laser-activated chitosan adhesive," *Lasers Surg. Med.* **39**, 19–27 (2007).
23. P. Chetoni et al., "Healing of rabbits' cornea following laser welding: effect of solid and semisolid formulations containing indocyanine green," *J. Drug Deliv. Sci. Technol.* **17**, 25–31 (2007).
24. B. V. Slaughter et al., "Hydrogels in regenerative medicine," *Adv. Mater.* **21**, 3307–3329 (2009).
25. J. M. Dang and K. W. Leong, "Natural polymers for gene delivery and tissue engineering," *Adv. Drug Deliv. Rev.* **58**, 487–499 (2006).
26. C. M. Shi et al., "Therapeutic potential of chitosan and its derivatives in regenerative medicine," *J. Surg. Res.* **133**, 185–192 (2006).
27. S. Bogni et al., "Tissue fusion, a new opportunity for sutureless bypass surgery," *Acta Neurochir. Suppl.* **112**, 45–53 (2011).
28. I. C. D. Wolf-de Jonge, J. F. Beek, and R. Balm, "25 years of laser assisted vascular anastomosis (LAVA): what have we learned?," *Eur. J. Vasc. Endovasc. Surg.* **27**, 466–476 (2004).
29. G. Esposito et al., "Present status and new perspectives in laser welding of vascular tissues," *J. Biol. Regul. Homeost. Agents* **25**, 145–152 (2011).
30. F. M. P. Leclere et al., "1.9 μm diode laser assisted vascular microanastomoses: experience in 40 clinical procedures," *Lasers Surg. Med.* **43**, 293–297 (2011).
31. L. Menabuoni et al., "Laser-assisted corneal welding in cataract surgery: retrospective study," *J. Cataract Refract. Surg.* **33**, 1608–1612 (2007).
32. V. Saxena, M. Sadoqi, and J. Shao, "Degradation kinetics of indocyanine green in aqueous solution," *J. Pharm. Sci.* **92**, 2090–2097 (2003).
33. W. Holzer et al., "Photostability and thermal stability of indocyanine green," *J. Photochem. Photobiol. B* **47**, 155–164 (1998).
34. J. Gathje, R. R. Steuer, and K. R. Nicholes, "Stability studies on indocyanine green dye," *J. Appl. Physiol.* **29**, 181–185 (1970).
35. J. Pauli et al., "An in vitro characterization study of new near infrared dyes for molecular imaging," *Eur. J. Med. Chem.* **44**, 3496–3503 (2009).
36. F. Ratto et al., "Gold nanorods as exogenous chromophores in the welding of ocular tissues," *Proc. SPIE* **6844**, 68441V (2008).
37. A. M. Gobin et al., "Near infrared laser-tissue welding using nanoshells as an exogenous absorber," *Lasers Surg. Med.* **37**, 123–129 (2005).
38. X. H. Huang et al., "Plasmonic photothermal therapy (PPTT) using gold nanoparticles," *Lasers Med. Sci.* **23**, 217–228 (2008).
39. M. C. Daniel and D. Astruc, "Gold nanoparticles: Assembly, supramolecular chemistry, quantum-size-related properties, and applications toward biology, catalysis, and nanotechnology," *Chem. Rev.* **104**, 293–346 (2004).
40. X. H. Huang, S. Neretina, and M. A. El-Sayed, "Gold Nanorods: from synthesis and properties to biological and biomedical applications," *Adv. Mater.* **21**, 4880–4910 (2009).
41. J. Perez-Juste et al., "Gold nanorods: synthesis, characterization and applications," *Coord. Chem. Rev.* **249**, 1870–1901 (2005).
42. P. K. Jain et al., "Calculated absorption and scattering properties of gold nanoparticles of different size, shape, and composition: Applications in biological imaging and biomedicine," *J. Phys. Chem. B* **110**, 7238–7248 (2006).
43. L. R. Hirsch et al., "Metal nanoshells," *Ann. Biomed. Eng.* **34**, 15–22 (2006).
44. F. Ratto et al., "Size and shape control in the overgrowth of gold nanorods," *J. Nanopart. Res.* **12**, 2029–2036 (2010).
45. S. J. Oldenburg et al., "Nanoengineering of optical resonances," *Chem. Phys. Lett.* **288**, 243–247 (1998).
46. A. M. Alkilany and C. J. Murphy, "Toxicity and cellular uptake of gold nanoparticles: what we have learned so far?," *J. Nanopart. Res.* **12**, 2313–2333 (2010).
47. N. G. Khlebtsov and L. A. Dykman, "Optical properties and biomedical applications of plasmonic nanoparticles," *J. Quant. Spectrosc. Radiat. Transfer* **111**, 1–35 (2010).
48. H. Wang et al., "Plasmonic nanostructures: artificial molecules," *Acc. Chem. Res.* **40**, 53–62 (2007).
49. A. A. Oraevsky et al., "Gold and silver nanoparticles as contrast agents for optoacoustic imaging," in *Photoacoustic imaging and spectroscopy*, L. V. Wang, Ed., pp. 373–386, CRC Press (2009).

50. C. J. Murphy et al., "Chemical sensing and imaging with metallic nanorods," *Chem. Commun.* **5**, 544–557 (2008).
51. A. M. Gobin et al., "Near-infrared resonant nanoshells for combined optical imaging and photothermal cancer therapy," *Nano Lett.* **7**, 1929–1934 (2007).
52. M. S. Nourbakhsh and M. E. Khosroshahi, "An in-vitro investigation of skin tissue soldering using gold nanoshells and diode laser," *Lasers Med. Sci.* **26**, 49–55 (2011).
53. F. Ratto et al., "Photothermal effects in connective tissues mediated by laser-activated gold nanorods," *J. Nanomed.* **5**, 143–151 (2009).
54. P. Matteini et al., "In vivo carotid artery closure by laser activation of hyaluronan-embedded gold nanorods," *J. Biomed. Opt.* **15** (4), 041508(2010).
55. P. Matteini et al., "Chitosan films doped with gold nanorods as laser-activatable hybrid bioadhesives," *Adv. Mater.* **22**, 4313 (2010).
56. B. Bregy et al., "Electromagnetic tissue fusion using superparamagnetic iron oxide nanoparticles: first experience with rabbit aorta," *Open Surg. J.* **2**, 3–9 (2008).
57. S. S. Chang et al., "The shape transition of gold nanorods," *Langmuir* **15**, 701–709 (1999).
58. S. Link and M. A. El-Sayed, "Shape and size dependence of radiative, non-radiative and photothermal properties of gold nanocrystals," *Int. Rev. Phys. Chem.* **19**, 409–453 (2000).
59. H. Petrova et al., "On the temperature stability of gold nanorods: comparison between thermal and ultrafast laser-induced heating," *Phys. Chem. Chem. Phys.* **8**, 814–821 (2006).
60. S. Inasawa, M. Sugiyama, and Y. Yamaguchi, "Laser-induced shape transformation of gold nanoparticles below the melting point: The effect of surface melting," *J. Phys. Chem. B* **109**, 3104–3111 (2005).
61. C. M. Aguirre et al., "Laser-induced reshaping of metallodielectric nanoshells under femtosecond and nanosecond plasmon resonant illumination," *J. Phys. Chem. B* **108**, 7040–7045 (2004).
62. Y. S. Chen et al., "Enhanced thermal stability of silica-coated gold nanorods for photoacoustic imaging and image-guided therapy," *Opt. Exp.* **18**, 8867–8878 (2010).
63. F. Ratto et al., "Stability of cetrimonium and silica modified gold nanorods/polyvinyl alcohol nano-composites upon near infrared laser excitation," *Proc. SPIE* **7577**, 757716 (2010).
64. L. C. Chen et al., "Enhanced photoacoustic stability of gold nanorods by silica matrix confinement," *J. Biomed. Opt.* **15** (2010).
65. Y. Liu, E. N. Mills, and R. J. Composto, "Tuning optical properties of gold nanorods in polymer films through thermal reshaping," *J. Mater. Chem.* **19**, 2704–2709 (2009).
66. Y. Khalavka et al., "Enhanced thermal stability of gold and silver nanorods by thin surface layers," *J. Phys. Chem. C* **111**, 12886–12889 (2007).
67. Y. Pan et al., "Size-dependent cytotoxicity of gold nanoparticles," *Small* **3**, 1941–1949 (2007).
68. M. Tsoli et al., "Cellular uptake and toxicity of Au(55) clusters," *Small* **1**, 841–844 (2005).
69. J. F. Hainfeld et al., "Gold nanoparticles: a new X-ray contrast agent," *Brit. J. Radiol.* **79**, 248–253 (2006).
70. H. S. Choi et al., "Renal clearance of quantum dots," *Nat. Biotechnol.* **25**, 1165–1170 (2007).
71. J. Perez-Juste et al., "Optical control and patterning of gold-nanorod-poly(vinyl alcohol) nanocomposite films," *Adv. Funct. Mater.* **15**, 1065–1071 (2005).
72. P. Zijlstra, J. W. M. Chon, and M. Gu, "Five-dimensional optical recording mediated by surface plasmons in gold nanorods," *Nature* **459**, 410–413 (2009).
73. S. Bogni et al., "Thermal model for optimization of vascular laser tissue soldering," *J. Biophotonics* **3**, 284–295 (2010).
74. A. Barak et al., "Temperature-controlled CO_2 laser tissue welding of ocular tissues," *Surv. Ophthalmol.* **42**, S77–S81 (1997).
75. F. Rossi, R. Pini, and L. Menabuoni, "Experimental and model analysis on the temperature dynamics during diode laser welding of the cornea," *J. Biomed. Opt.* **12**(1), 014031 (2007).
76. G. Esposito et al., "An experimental study on minimally occlusive laser-assisted vascular anastomosis in bypass surgery: The importance of temperature monitoring during laser welding procedures," *J. Biol. Regul. Homeost. Agents* **24**, 307–315 (2010).
77. M. H. Niemz, *Laser-tissue interactions: fundamentals and applications*, Springer, Berlin (2007).
78. S. Thomsen, "Pathologic analysis of photothermal and photomecanical effects of laser-tissue interactions," *Photochem. Photob.* **53**, 825–835 (1991).
79. V. Rieke and K. B. Pauly, "MR thermometry," *J. Magn. Reson. Imaging* **27**, 376–390 (2008).
80. R. Maass-Moreno and C. A. Damianou, "Noninvasive temperature estimation in tissue via ultrasound echo-shifts. Part I. Analytical model," *J. Acoust. Soc. Am.* **100**, 2514–2521 (1996).
81. T. Patterson, M. M. Stecker, and B. L. Netherton, "Mechanisms of electrode induced injury. Part 2: Clinical experience," *Am. J. Electroneurodiagnostic Technol.* **47**, 93–113 (2007).
82. P. T. Hardy and K. M. Weil, "A review of thermal MR injuries," *Radiol. Technol.* **81**, 606–609 (2010).
83. I. Bazan et al., "A performance analysis of echographic ultrasonic techniques for non-invasive temperature estimation in hyperthermia range using phantoms with scatterers," *Ultrasonics* **49**, 358–376 (2009).
84. A. A. Oraevsky et al., "Laser-Based Optoacoustic Imaging in Biological Tissues," *Proc. SPIE* **2134**, 122–128 (1994).
85. C. Li and L. V. Wang, "Photoacoustic tomography and sensing in biomedicine," *Phys. Med. Biol.* **54**, R59–97 (2009).
86. L. V. Wang, "Prospects of photoacoustic tomography," *Med. Phys.* **35**, 5758–5767 (2008).
87. M. X. Tang et al., "Photoacoustics, thermoacoustics, and acousto-optics for biomedical imaging," *Proc. Inst. Mech. Eng. H* **224**, 291–306 (2010).
88. R. O. Esenaliev, A. A. Karabutov, and A. A. Oraevsky, "Sensitivity of laser opto-acoustic imaging in detection of small deeply embedded tumors," *J. IEEE Sel. Top. Quant.* **5**, 981–988 (1999).
89. S. A. Ermilov et al., "Laser optoacoustic imaging system for detection of breast cancer," *J. Biomed. Opt.* **14**, 024007 (2009).
90. S. Mallidi et al., "Molecular specific optoacoustic imaging with plasmonic nanoparticles," *Opt. Exp.* **15**, 6583–6588 (2007).
91. J. Shah et al., "Photoacoustic imaging and temperature measurement for photothermal cancer therapy," *J. Biomed. Opt.* **13**, 034024 (2008).
92. M. Pramanik and L. V. Wang, "Thermoacoustic and photoacoustic sensing of temperature," *J. Biomed. Opt.* **14**, 054024 (2009).
93. G. Schule et al., "Noninvasive optoacoustic temperature determination at the fundus of the eye during laser irradiation," *J. Biomed. Opt.* **9**, 173–179 (2004).
94. J. Kandulla, H. Elsner, R. Birngruber, and R. Brinkmann, "Noninvasive optoacoustic online retinal temperature determination during continuous-wave laser irradiation," *J. Biomed. Opt.* **11**, 041111 (2006).
95. X. Yang et al., "Nanoparticles for photoacoustic imaging," *Wiley Interdiscip. Rev. Nanomed. Nanobiotechnol.* **1**, 360–368 (2009).
96. S. Egerev et al., "Acoustic signals generated by laser-irradiated metal nanoparticles," *Appl. Opt.* **48**, C38–C45 (2009).
97. L. Tong et al., "Gold nanorods as contrast agents for biological imaging: optical properties, surface conjugation and photothermal effects," *Photochem. Photob.* **85**, 21–32 (2009).
98. S. Link, M. B. Mohamed, and M. A. El-Sayed, "Simulation of the optical absorption spectra of gold nanorods as a function of their aspect ratio and the effect of the medium dielectric constant," *J. Phys. Chem. B* **103**, 3073–3077 (1999).
99. L. Qiu et al., "Gold nanorod light scattering labels for biomedical imaging," *Biomed. Opt. Exp.* **1**, 135–142 (2010).
100. N. G. Khlebtsov, "Anisotropic properties of plasmonic nanoparticles: depolarized light scattering, dichroism, and birefringence," *J. Nanophotonics* **4**, 041587 (2010).
101. P. G. Etchegoin, E. C. Le Ru, and M. Meyer, "An analytic model for the optical properties of gold," *J. Chem Phys.* **125**, 164705 (2006).
102. D. Huang et al., "Optical coherence tomography," *Science* **254**, 1178–1181 (1991).
103. C. Loo et al., "Immunotargeted nanoshells for integrated cancer imaging and therapy," *Nano Lett.* **5**, 709–711 (2005).
104. A. L. Oldenburg et al., "Plasmon-resonant gold nanorods as low backscattering albedo contrast agents for optical coherence tomography," *Opt. Exp.* **14**, 6724–6738 (2006).

105. G. Sonavane et al., "In vitro permeation of gold nanoparticles through rat skin and rat intestine: Effect of particle size," *Colloids Surf. B Biointerfaces* **65**, 1–10 (2008).
106. E. A. Genina et al., "In vitro study of Indocyanine Green solution interaction with skin," *Proc. SPIE* **6535**, 65351H (2007).
107. J. W. Stone et al., "Using gold nanorods to probe cell-induced collagen deformation," *Nano Lett.* **7**, 116–119 (2007).
108. C. G. Wilson et al., "Glycosaminoglycan-functionalized gold nanorods: interactions with cardiac cells and type I collagen," *J. Mater. Chem.* **19**, 6332–6340 (2009).